SMM Behaviour and Magnetocaloric Effect in Heterometallic 3*d*-4*f* Coordination Clusters with High Azide:Metal Ratios

Sebastian F. M. Schmidt,[a] Marcel P. Merkel,[d] George E. Kostakis,[b] Gernot Buth,[c] Christopher E. Anson[a] and Annie K. Powell [a,d]

Experimental section

General Procedures.

Unless otherwise stated, all reagents were obtained from commercial sources and were used as received without further purification. The synthesis of complex **6** has been previously described.[32] All reactions were carried out under aerobic conditions. Elemental analyses (CHN) were performed using an Elementar Vario EL Analyzer. FTIR spectra were measured as KBr pellets over 4000-400 cm^{-1} on a Perkin Elmer *Spectrum One* spectrometer. *Caution! Although no such tendency was observed during the present work, azide salts are potentially explosive and should be handled with care and in small quantities.*

Synthesis of Azidometallates

The synthesis of homoleptic azidometallates often involves the use of silverazide in combination with metal halogenides or metal fluorides in combination with trimethylsilylazides. We developed an easier and quicker approach to synthesise the desired azidometalates in high yields. It involves the use of metalchlorides with sodium azide and a bulky cation in a two phasic system of water and dichloromethane. *Caution! Mixtures of sodium azide with dichloromethane and a phase transfer reagent can contain diazidomethane which is very explosive. These reaction conditions should be maintained only shortly and the mixture should be handled with care and in small quantities.* It is possible to obtain crystalline products in this way (**3**). But we found that the desired heterometallic products in this work can only be obtained with tetrabutyl ammonium cations. The corresponding azidometalates of iron and manganese are oils in this case. Their elemental analysis is pointing to $Fe(N_3)_5^{2-}$ and $Mn(N_3)_6^{3-}$ anions.

Synthesis of $[P(Ph)_4]_2[Fe(N_3)_5]$ 3

1 mmol of $FeCl_3{\cdot}6H_2O$ is dissolved in 2 mL of water. 2 mmol of tetraphenylphosphonium bromide and 5 mmol of NaN_3 are dissolved in water and layered with 10 ml of dichloromethane. Under vigorous stirring the solution of the metal chloride is added. After one minute the organic layer is separated, dried over calcium chloride and evaporated under ambient conditions to obtain the deep red product. Yield: 73% relative to $FeCl_3{\cdot}6H_2O$. *Anal.* calculated C 61.02, H 4.27, N 22.24; found: C 61.13, H 4.346, N 22.24 IR (KBr) /cm^{-1}: 3422(br), 2042(s), 1435(m), 1327(m), 1105(s), 995(m), 759(m), 523(vs)

Synthesis of $[TBA]_2[Fe(N_3)_5]$

The synthesis of this compound was carried out in the same way as **3**. Tetrabutylammonium bromide was used instead of tetraphenylphosphonium bromide. Yield of the deep red oil: 84 % relative to $FeCl_3{\cdot}6H_2O$. *Anal.* Calculated C 51.19, H 9.67, N 31.71; found C 50.89, H 9.98, N 30.65 IR (KBr) /cm^{-1}: 2962(s), 2037(s), 2011(m), 1471(s)

Synthesis of $[TBA]_2[Mn(N_3)_6]$

The synthesis of this compound was carried out in the same way as **3**. $MnCl_2{\cdot}6H_2O$ was used instead of $FeCl_3{\cdot}6H_2O$, tetrabutylammonium bromide was used instead of tetraphenylphosphonium bromide and the reaction time was increased to two hours to allow for the oxidation of manganese. Yield of the brown oil: 96 % relative to $MnCl_2{\cdot}6H_2O$ *Anal.* Calculated C 55.73, H 10.52, N 28.43; found C 56.19, H 10.1, N 28.12 IR (KBr) /cm^{-1}: 2943(s), 2048(s), 1485(s)

Synthesis of heterometallic compounds

$$Fe(N_3)_5^{2-} \xrightarrow{\text{tipa}H_3,\ Gd(NO_3)_3{\cdot}x(H_2O)} [Fe_3Gd_2(N_3)_{15}(OH)_3(\text{tipa}H_3)_2]^{3-} \quad \mathbf{1}$$

$$Mn(N_3)_6^{2-} \xrightarrow{\text{tea}H_3,\ Dy(NO_3)_3{\cdot}x(H_2O)} [Mn_4Dy_2(N_3)_{12}(\text{tea}H_2)_4]^{2-} \quad \mathbf{2}$$

$\text{tipa}H_3$ = triisopropanolamine; $\text{tea}H_3$ = triethanolamine;

Synthesis of $(TBA)_3[Fe_3Gd_2(N_3)_{15}(OH)_3(\text{tipa}H_3)_2]$ 1

1 mmol of $FeCl_3{\cdot}6H_2O$ is dissolved in 2 mL of water. 2 mmol of tetrabutylammonium bromide and 5 mmol of NaN_3 are dissolved in water and layered with 10 ml of dichloromethane. Under vigorous stirring the solution of the metal chloride is added. After one minute the organic layer is separated and dried over calcium chloride. The dichloromethane solution is then added dropwise to an ethanolic solution 1 mmol of triisopropanolamine and 0.5 mmol of $Gd(NO_3)_3{\cdot}xH_2O$. Yield of dark red crystals: 7 % relative to $Gd(NO_3)_3{\cdot}xH_2O$. *Anal.* Calculated C 34.78, H 6.78, N 30.81; found C 34.75, H 6.74, N 30.53 IR (KBr) /cm^{-1}: 3393 (bm), 2864 (s), 2095 (s), 2067 (s), 2054 (s), 1548 (s), 1418 (s), 1074 (s), 847 (s)

Synthesis of $(TBA)_2[Mn_4Dy_2(N_3)_{12}(\text{tea}H_2)_4]$ 2

1 mmol of $MnCl_2{\cdot}6H_2O$ is dissolved in 2 mL of water. 2 mmol of tetrabutylammonium bromide and 5 mmol of NaN_3 are dissolved in water and layered with 10 ml of dichloromethane. Under vigorous stirring the solution of the metal chloride is added. After two hours the organic layer is separated and dried over calcium chloride. The dichloromethane solution is then added dropwise to an ethanolic solution of 1 mmol of triethanolamine and 0.5 mmol of $Dy(NO_3)_3{\cdot}xH_2O$. Yield of black crystals: 12 % relative to $Dy(NO_3)_3{\cdot}xH_2O$ *Anal.* Calculated C: 31.69; H: 5.89; N: 27.71; found C 31.62, H 5.86 N 27.74 IR (KBr) /cm^{-1}: 3391 (bm), 2845 (s), 2073 (s), 2023 (s), 1567 (s), 1386 (s), 694 (s)

Crystallography

Data for **1** and **2** were measured at 150(2) K with a Bruker SMART Apex diffractometer on the SCD beamline at the ANKA synchrotron source, Karlsruhe Institute of Technology, using Si-monochromated radiation of wavelength 0.80039 Å. Data for **3** were collected at 223(2) K with a Stoe IPDS diffractometer using graphite-monochromated Mo-Kα radiation. Datasets were corrected for polarisation and absorption effects. The crystal of **2** was found to be moderately twinned (minor component ca. 21%) by a 180 deg rotation about *a**. The data were integrated and corrected for absorption taking this twinning into account. Crystals of **3** were of poor quality, and no significant intensity could be measured for $2\theta > 46.5°$; the data were therefore truncated at this point. Since **3** is only a precursor complex, no attempt was made to re-collect data using the synchrotron source.

Structure solution by direct methods using SHELXS[x1] was followed by full-matrix least-squares refinement using SHELXL-2016[x2], with anisotropic thermal parameters for all ordered non-H atoms. O-H distances were restrained to 0.88(4) Å; organic H-atoms were placed in calculated positions. For the structures of **1** and **2**, anomalous scattering factors f′ and f″ were calculated using the method of Brennan and Cowan[x3], as implemented on http://skuld.bmsc.washington.edu/scatter/AS_periodic.html.

Disorder in the n-butyl groups of the cations and in the lattice solvent was modelled using pairs of partial-occupancy isotropic atoms and geometrical similarity restraints as appropriate. In the structure of **1**, a lattice CH_2Cl_2 and C_2H_5OH were mutually (and badly) disordered over an inversion centre. The contributions of these to the structure calculations was calculated using SQUEEZE[x4], as implemented in PLATON[x5]. The atoms of these disordered ("SQUEEZEd") molecules are included in the SFAC/UNIT list. Structure factors in the refinement included these contributions from the .fab file.

Crystallographic data for the structures in this paper have been deposited with the Cambridge Crystallographic Data Centre as supplementary publication nos. CCDC 1559987-1559989. Copies of the data can be obtained, free of charge, from https://summary.ccdc.cam.ac.uk/structure-summary-form.

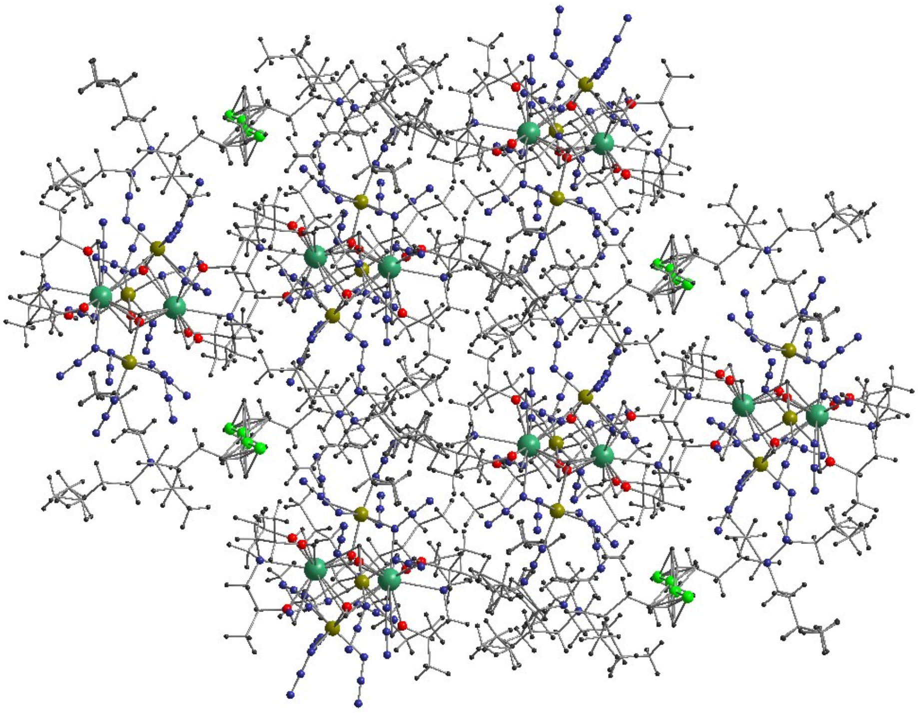

Figure S1 Packing diagram of the crystal structure of **1**

Table S1 Selected bond distances of **1**

Atom1	Atom2	Distance [Å]	Atom1	Atom2	Distance [Å]
Gd1	O6	2.4086(19)	Fe1	N61	1.990(3)
Gd1	O1	2.4217(17)	Fe1	N51	2.053(2)
Gd1	O4	2.4372(19)	Fe1	O1	2.0655(16)
Gd1	O2	2.4389(17)	Fe1	N11	2.085(2)
Gd1	O5	2.4435(17)	Fe1	N81	2.087(3)
Gd1	O3	2.4730(17)	Fe1	N71	2.111(3)
Gd1	N21	2.548(2)	Fe2	N101	2.030(2)
Gd1	N1	2.789(2)	Fe2	N91	2.044(2)
Gd2	O3	2.3975(17)	Fe2	N121	2.066(2)
Gd2	O8	2.4035(18)	Fe2	N111	2.078(2)
Gd2	O9	2.4380(18)	Fe2	O2	2.0865(16)
Gd2	O7	2.4498(19)	Fe2	N21	2.099(2)
Gd2	O2	2.4618(16)	Fe3	N151	1.993(2)
Gd2	O1	2.4876(17)	Fe3	N31	2.048(2)
Gd2	N11	2.526(2)	Fe3	N131	2.065(2)
Gd2	N41	2.597(2)	Fe3	N141	2.067(3)
Gd2	N2	2.744(2)	Fe3	O3	2.0766(18)
			Fe3	N41	2.146(2)

Table S2 Selected bond angles of **1**

Atom13	Atom23	Atom3	Angle [°]
Gd1	O1	Gd2	96.74(6)
Gd1	O2	Gd2	96.98(6)
Gd1	O3	Gd2	97.77(6)
Fe1	O1	Gd2	108.83(7)
Fe1	O1	Gd1	119.69(8)
Fe2	O2	Gd2	124.68(8)
Fe2	O2	Gd1	109.28(7)
Fe3	O3	Gd2	112.33(7)
Fe3	O3	Gd1	115.01(7)
Fe1	N11	Gd2	106.80(8)
Fe2	N21	Gd1	104.97(8)
Fe3	N31	Gd1	101.99(10)
Fe3	N41	Gd2	102.94(8)

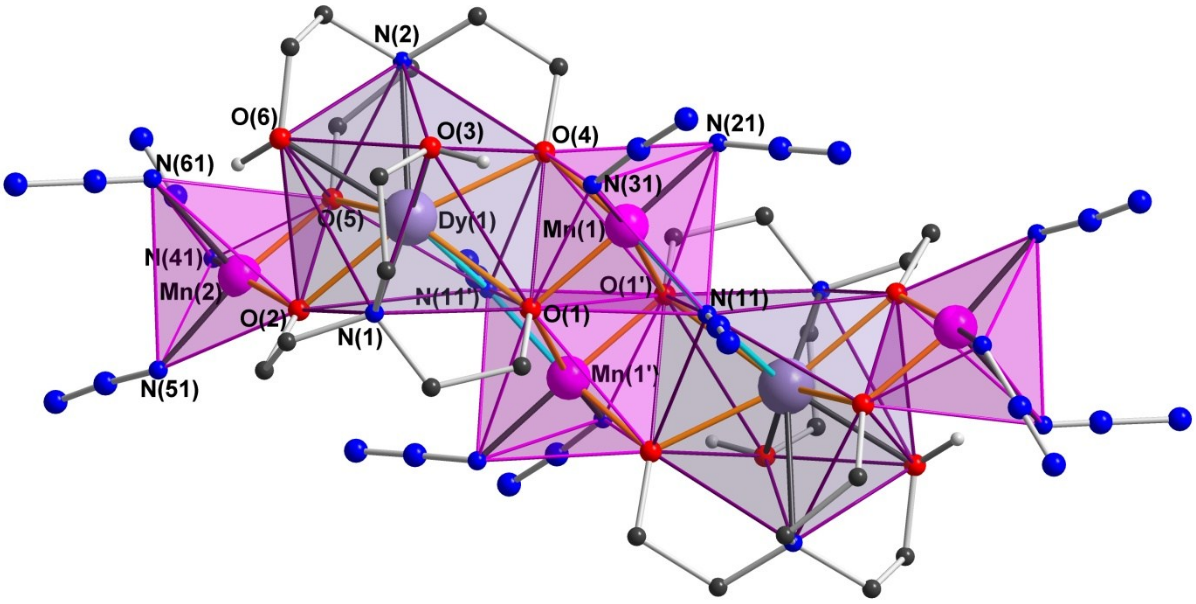

Figure S2: Structure of cluster anion in **2** showing coordination polyhedra.

Table S3 Selected bond distances of **2**

Atom1	Atom2	Abstand [Å]	Atom1	Atom2	Abstand [Å]
Dy1	O2	2.291(6)	Mn1	O4	1.923(5)
Dy1	O4	2.364(5)	Mn1	N21	1.946(7)
Dy1	O5	2.380(5)	Mn1	N11	1.986(6)
Dy1	O1	2.488(5)	Mn1	O1	1.998(5)
Dy1	O3	2.491(6)	Mn1	N31	2.187(7)
Dy1	O6	2.491(6)	Mn1	O1	2.353(5)
Dy1	N11	2.581(6)	Mn2	O5	1.895(5)
Dy1	N2	2.599(7)	Mn2	N41	1.943(7)
Dy1	N1	2.642(7)	Mn2	O2	1.950(6)
Dy1	Mn2	3.4577(13)	Mn2	N51	1.954(7)
Dy1	Mn1	3.5132(12)	Mn2	N61	2.256(10)

Table S4 Selected bond angles of **2**

Atom1	Atom2	Atom3	Winkel [°]
Mn1	O1	Dy1	102.6(2)
Mn1	O1	Dy1	103.13(17)
Mn1	O4	Dy1	109.6(2)
Mn1	O1	Mn1	98.56(18)
Mn2	O2	Dy1	109.0(2)
Mn2	O5	Dy1	107.4(2)
Mn1	N11	Dy1	111.7(3)

Table S5 Crystallograpic data of **1**, **2** and **3**

	1	**2**	**3**
Sum formula	$C_{68}H_{158}Cl_2Fe_3Gd_2N_{50}O_{9.5}$	$C_{56}H_{124}Dy_2Mn_4N_{42}O_{12}$	$C_{48}H_{40}FeN_{15}P_2$
FW [g/mol]	2381.39	2122.73	944.74
Temperature [K]	150(2)	150(2)	223(2)
Crystal system	triclinic	monoclinic	Monoclinic
Space group	$P\bar{1}$	$P2_1/c$	C2/c
a [Å]	16.989(2)	17.178(4)	11.7369(15)
b [Å]	17.111(2)	15.074(4)	18.103(2)
c [Å]	22.479(3)	17.795(4)	21.962(3)
α [°]	68.741(2)	90	90
β [°]	80.570(2)	93.283(4)	91.789(15)
g [°]	63.397(2)	90	90
V [$Å^3$]	5445.3(13)	4600.3(18)	4664.1(11)
Z	2	2	4
ρ [g/cm^3]	1.452	1.532	1.345
μ [mm^{-1}]	2.319	3.028	0.444
F(000)	2464	2164	1956
T [K]	150(2)	150(2)	223(2)
λ [Å]	0.80039	0.80039	0.71073
Data measured	104884	56288	13012
R(int)	0.0468	0.0597	0.1067
Independent data	23862	9750	3249
Ind. Data with $I > 2\sigma(I)$	20789	8350	1990
Refined parameters	1225	528	312
S (all data)	1.052	1.084	0.918
wR_2 (all data)	0.0755	0.1794	0.1023
R_1 [$I>2\sigma(I)$]	0.0292	0.0705	0.0441
Min/max electron density [e $Å^{-3}$]	1.4x/-1.16	2.47/-1.49	0.19 / -0.37
CCDC	1559987	1559988	1559989

Magnetic measurements

Magnetic susceptibility data (2-300K) were collected on powdered polycrystalline samples on a Quantum Design MPMS-XL SQUID magnetometer under an applied magnetic field of 0.1 T. *Ac* measurements were performed in the 2-10K range using a 3.0 Oe *ac* field oscillation in 1-1500Hz range. Magnetization isotherms were collected at 2K between 0 and 5T. All data were corrected from the sample holder contribution and the diamagnetism of the samples estimated from Pascal's constants.[36,37]

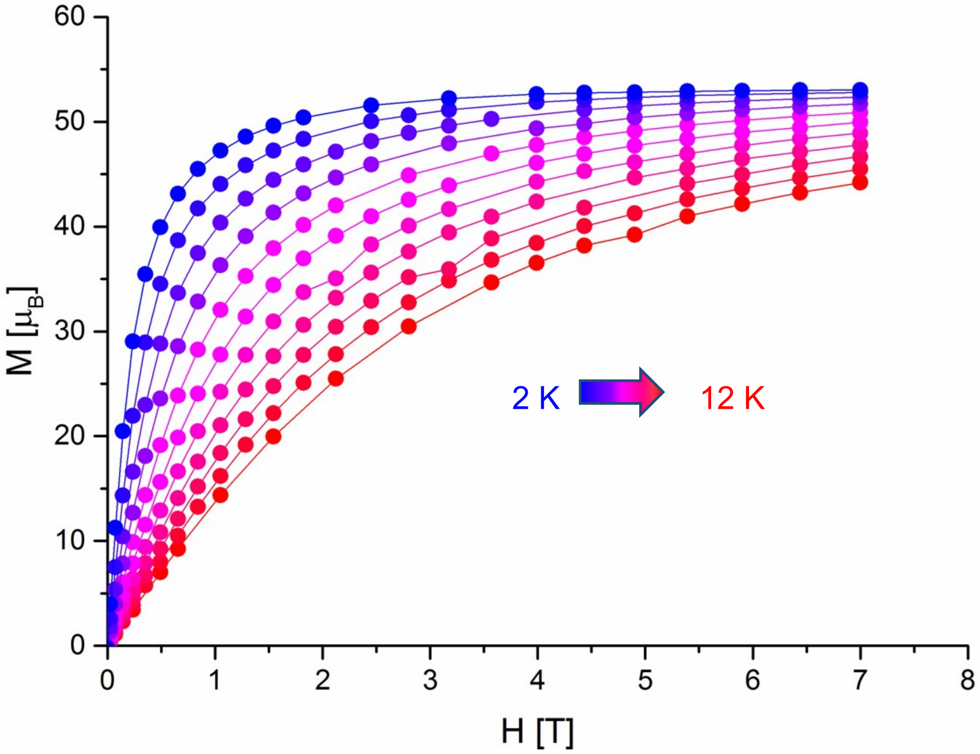

Figure S3 magnetisation in the dependence of the magnetic field of **1** in a temperature range of 2 to 12 K

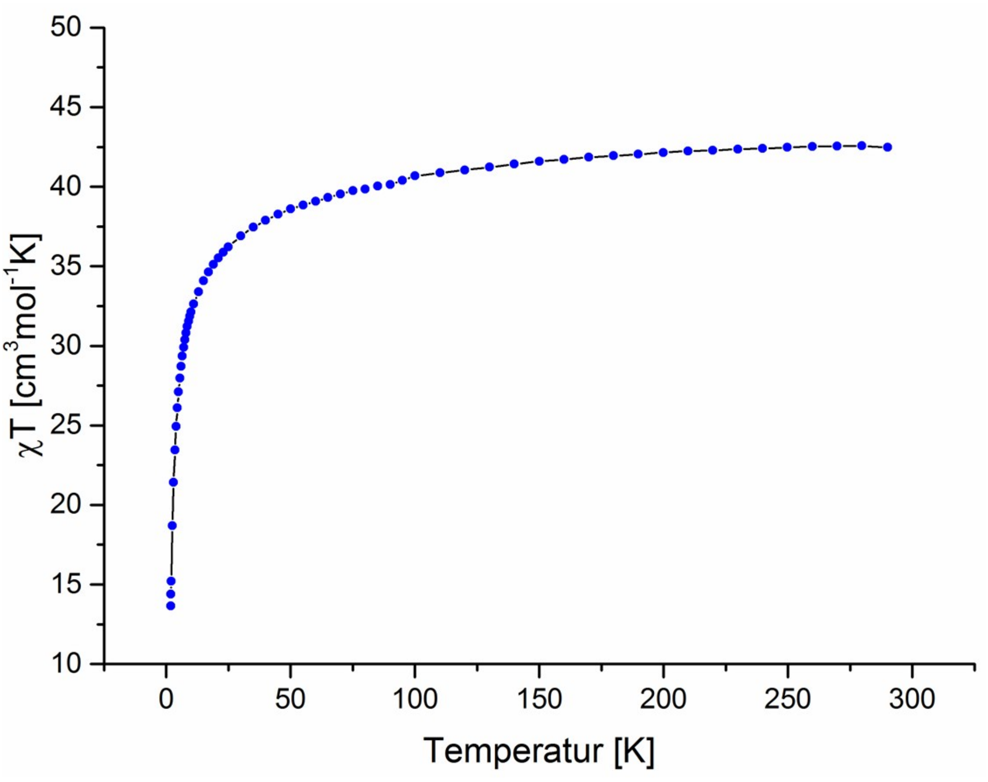

Figure S4 χT vs T of **2** between 2 and 300 K and an applied field of 0.1 T

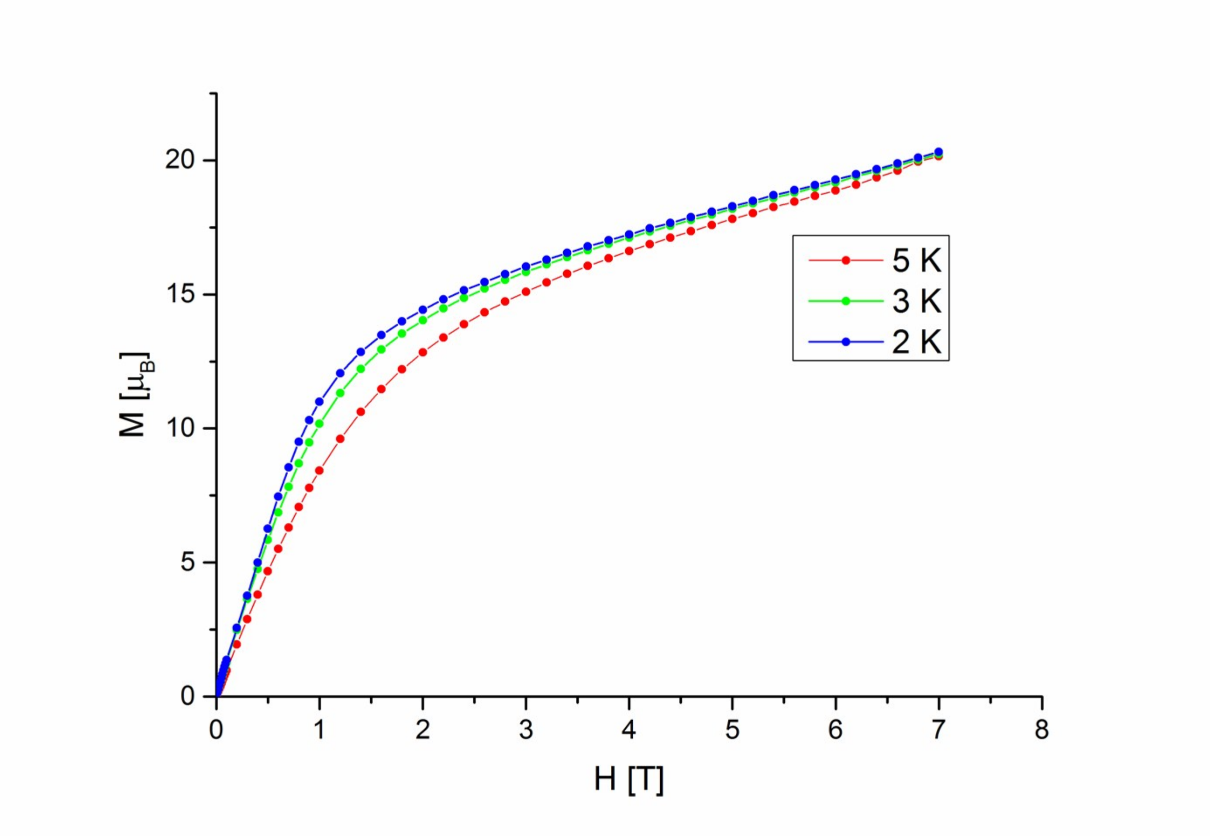

Figure S5 magnetisation in the dependence of the magnetic field of **2** in a temperature range of 3 to 5 K

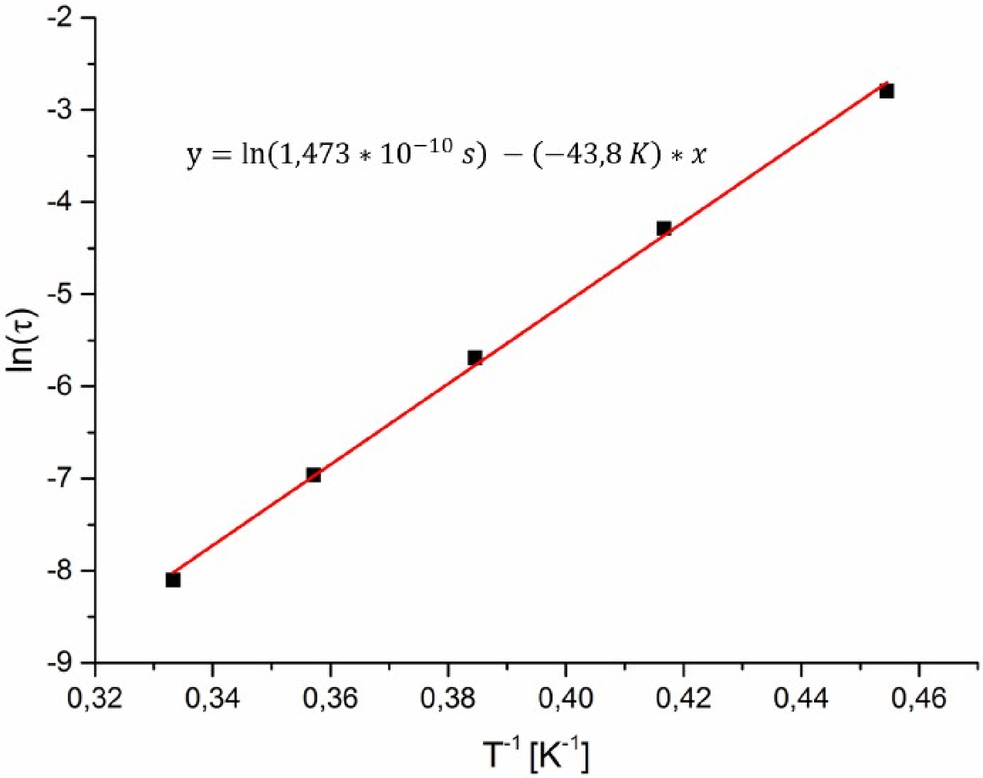

Figure S6 Arrhenius Plot of **2**

[1] G.M. Sheldrick, *Acta Cryst.*, 2008, **A64**, 112-122

[2] G.M. Sheldrick, *Acta Cryst.*, 2015, **C71**, 3-8

[3] S Brennan and P.L. Cowan, *Rev. Sci. Instrum.*, 1992, **63**, 850

[4] A. L. Spek, *Acta Cryst.*, 2015, **C71**, 9-18

[5] A. L. Spek, *Acta Cryst.*, 2009, *D65*, 148-155